Electronic Supplementary Information (ESI)

Smart wormlike micelles switched by CO_2 and air

Yongmin Zhang,[a,c] Zonglin Chu,[a,c] Cécile A. Dreiss,[c] Yuejiao Wang,[a,c] Chenhong Fei,[a,c] and Yujun Feng*[a]

[a] *Chengdu Institute of Organic Chemistry, Chinese Academy of Sciences, Chengdu 610041, P. R. China. E-mail: yjfeng@cioc.ac.cn*

[b] *Institute of Pharmaceutical Science, King's College London, UK SE1 9NH*

[c] *University of the Chinese Academy of Sciences, Beijing 100049, People's Republic of China*

Experimental details

Materials. N-erucamidopropyl-N, N-dimethylamine (UC22AMPM) with purity greater than 99.0 % (HPLC) was synthesized according to our previously reported procedure.[1] Glucono-δ-lactone (Sigma-Aldrich, ≥ 99.0%), pyrene (Sigma-Aldrich, GC, ≥ 99.0%) and CO_2 (≥ 99.998%) were used without further purification. Water was triply distilled by a quartz water purification system. All other reagents used in the experiments were of analytical grade.

Sample Preparation. Specific amounts of UC22AMPM and distilled water were introduced into a glass vial sealed with rubber septa. CO_2 was bubbled at ambient temperature (25 °C) and pressure (0.1 MPa) at a fixed flow rate of 0.1 L·min^{-1} under continuous agitation, leading to a transparent viscoelastic fluid (referred to as "UC22AMPM-CO_2"). After that, the sample was kept in a sealed vessel to cut off from air. To efficiently remove CO_2, air was bubbled into 10 mL of UC22AMPM-CO_2 at ambient temperature until equilibrium at a flow rate of 0.1 L·min^{-1}, resulting in a low viscosity emulsion-like system (referred to as "UC22AMPM-air"). All the samples obtained were kept at 25 °C for about 24 h prior to the measurements.

Rheology. Rheological measurements were performed on a Physica MCR 301 (Anton Paar, Austria) rotational rheometer equipped with CC27 (ISO3219) concentric cylinder geometry with a measuring bob radius of 13.33 mm and a measuring cup radius of 14.46 mm. Samples were equilibrated at 25 °C for no less than 20 min prior to the experiments. Dynamic frequency spectra were conducted in the linear viscoelastic region, as determined from prior dynamic stress sweep measurements. All measurements were carried out in the stress-controlled mode, and CANNON standard oil was used to calibrate the instrument before the measurements. The temperature was controlled by a Peltier device, and a solvent trap was used to minimize water evaporation during the measurements.

Cryo-TEM observation. The specimens for cryo-TEM observation were prepared in a controlled environment to vitrify the solutions. The temperature of the chamber was regulated between 25 and 28 °C, and the relative humidity was kept close to saturation to prevent evaporation during the preparation. 5 μL of solution pre-heated at 25 °C was placed on a carbon-coated holey film supported by a copper grid, and gently blotted with filter paper to obtain a thin liquid film (20−400 nm) on the grid. Next, the grid was quenched rapidly into a cryogen reservoir containing liquid ethane at −180 °C and transferred into liquid nitrogen (−196 °C) for storage. Then the vitrified specimen stored in liquid nitrogen was transferred into a JEM2010 cryo-microscope using a Gatan 626 cryo-holder and its workstation. The acceleration voltage was set to 200 kV, and the working temperature was kept below −170 °C. The images were recorded digitally with a charge-coupled device camera (Gatan 832) under low-dose conditions with an under-focus of approximately 3 μm.

NMR spectroscopy. ^{1}H NMR and ^{13}C NMR spectra were recorded at 25 °C on a Bruker AV300 NMR spectrometer at 300 MHz and 75 MHz, respectively. Two parts of UC22AMPM with the same quantity were dissolved in CD_3OD/D_2O (v/v=5:1), respectively, and then one of them was treated with CO_2 at ambient temperature for 5 min with the flow rate of 0.05 L·min^{-1}. Chemical shifts (δ) are reported in parts per million (ppm) with reference to the internal standard protons of tetramethylsilane (TMS).

UV Absorbance measurements with Nile red. Triplicates of 1 mL solutions of 5 mM Nile red in acetone were injected into 10 mL distilled water in three cuvettes (A, B, and C), respectively, and then ultrasonicated for 30 min to remove the acetone. 42.2 mg UC22AMPM were added to each cuvette. After stirring at room temperature for 6 h and standing overnight, solutions B and C were slowly treated with CO_2 to equilibrium as described above, following which air was bubbled into sample C until equilibrium. Finally, solutions A, B and C were centrifuged for 10 min at 10,000 rpm, and the supernatant was recovered for absorbance measurement.

The absorbance of the solutions was measured on a double-beam UV-4802 UV-vis spectrophotometer (Unico, USA) at a temperature of 25 °C, which was controlled by a circulating water bath, over the wavelength range 300−900 nm. Pure water with Nile red was used as a reference.

pH measurement. The pH of a 100 mM UC22AMPM aqueous solution with bubbling CO_2 was monitored by a Sartorius basic pH-meter PB-10 (± 0.01) at 25 °C. The gas flow rate was fixed at 0.1 L/min. The variation of pH of pure water under bubbling CO_2 at 25 °C was also recorded as a reference.

Conductivity measurement. The conductivity of a 100 mM UC22AMPM aqueous solution with bubbling CO_2 was monitored by a FE30 conductometer (Mettler Toledo, USA) at 25 °C, and average values were calculated from three repeats. The gas flow rate was fixed at 0.1 L·min^{-1}. The conductivity of pure water under bubbling CO_2 at 25 °C was also determined as a reference.

Determination of the critical micellar concentration by

fluorescence spectroscopy. The critical micellar concentration (cmc) of UC22AMPM-CO_2 was measured using a Varian Cary Eclipse spectrometer (Varian Inc. USA). The temperature of the cell holder was controlled by a Neslab circulating water bath. The fluorescence emission spectra were recorded from 350 to 500 nm. The excitation wavelength was set at 335 nm, and the excitation and emission slit widths were set g 10 and 2.5 nm, respectively. First, a concentrated UC22AMPM-CO_2 was prepared with pyrene-saturated distilled water, and then a series of solutions were prepared by diluting determined amounts of concentrated UC22AMPM-CO_2 solutions with pyrene-saturated distilled water. All the measurements were performed at 25 °C.

Additional Results

2.1 Rheological parameters of UC22AMPM-CO_2

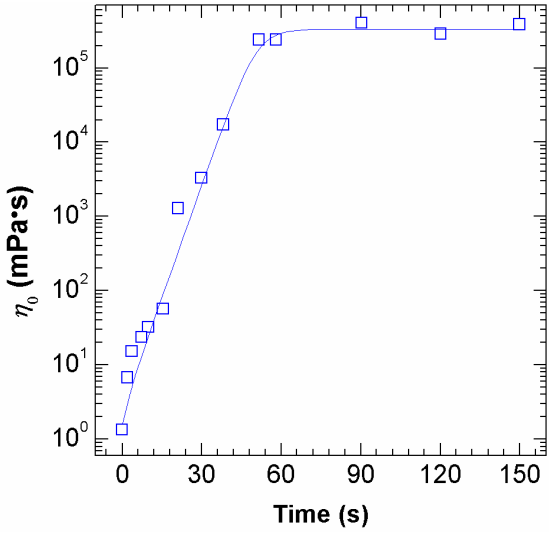

Fig. S1 Evolution of the zero-shear viscosity over time of a 20 mL solution of 100 mM UC22AMPM under CO_2 bubbling at a flow rate of ~0.1 L·min^{-1}.

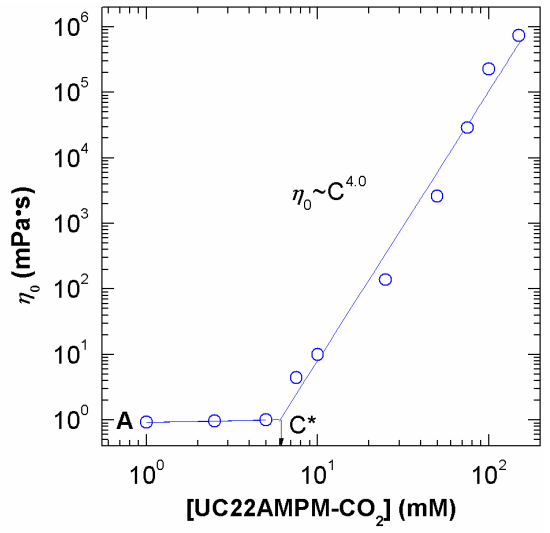

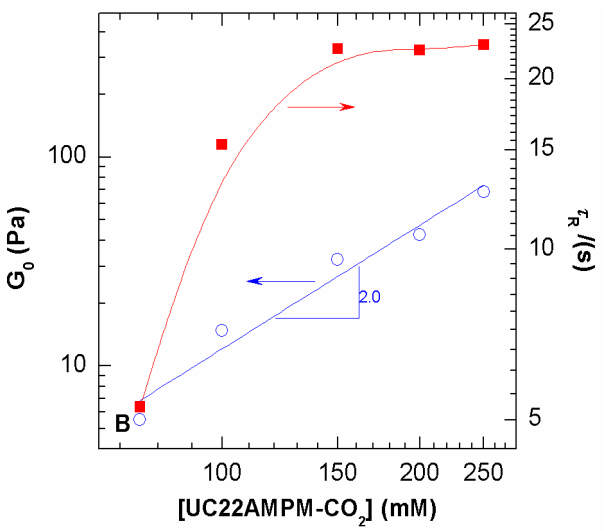

Fig. S2 Effect of UC22AMPM-CO_2 concentration on (A) zero-shear viscosity (η_0), (B) plateau modulus (G_0) and relaxation time (τ_R) at 25 °C.

Fig. S2 shows the rheological parameters plotted as a function of UC22AMPM-CO_2 concentration (C) at 25 °C. The η_0–C curve (Fig. S2A) can be divided into two parts, with a clear break-point, i.e., the overlapping concentration C^* (~6 mM). In the dilute regime ($C<C^*$), the average micellar length usually increases with surfactant concentration following a simple power-law model with an exponent of ~1/2, and the zero-shear viscosity (η_0) varies linearly with C following the Einstein equation:

$$\eta_0 = \eta_{water}(1 + KC) \qquad (1)$$

where K is of the order of unity.[2] When above C^*, the wormlike micelles start entangling, forming a dynamic transient network, which imparts substantial viscoelasticity to the solution,[3] and η_0 increases exponentially by several orders of magnitude, following the scaling law $\eta_0 \sim C^n$,[4] and the power-law exponent n is 4.0, slightly higher than the value of 3.5 predicted by the theoretical model for conventional wormlike micellar solutions.[5]

Exhibited in Fig. S2B are τ_R and G_0 plotted against UC22AMPM-CO_2 concentration. The maximum relaxation time quickly rises and then levels off upon increasing surfactant concentration. The plateau modulus G_0 rises steadily with surfactant concentration and exhibits a power-law behaviour: $G_0 \sim C^{2.0}$, with a value of the exponent close to that found for EDAS,[3] EHAC (erucyl bis-(hydroxyethyl) methylammonium chloride[6] and NaOEr-TMAB (sodium erucate-tetramethyl ammonium bromide).[7] An increase in these rheological parameters is due to the growth in the length of the wormlike micelles.[8] Upon an increase in surfactant concentration, micellar length and flexibility rise, leading to an increase in η_0 and τ_R. The increase in G_0 correlates to a concomitant increase in network mesh size.[9]

2.2 Appearance and steady rheology of UC22AMPM-CO_2 after six months

Electronic Supplementary Information (ESI)

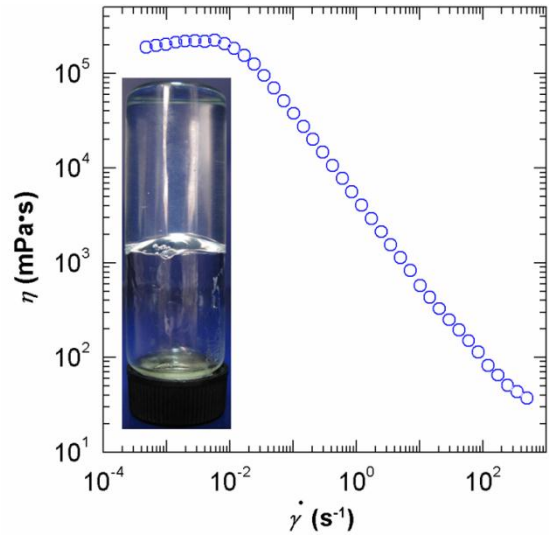

Fig. S3 Snapshot and steady rheology of UC22AMPM-CO_2 after being kept in a sealed vessel for 6 months.

As shown in Fig. S3, when UC22AMPM-CO_2 solution was kept in a sealed vessel for six months, it still appears as a transparent viscoelastic fluid. The zero-shear viscosity is as high as 280,000 mPa·s, very close to the initial value of UC22AMPM-CO_2 presented in Figure 1A. Compared with the sample in Figure 1A, the only difference is that those bubbles trapped in solution disappeared after half a year of storage.

2.3 Effect of CO_2 and air bubbling time on pH and conductivity

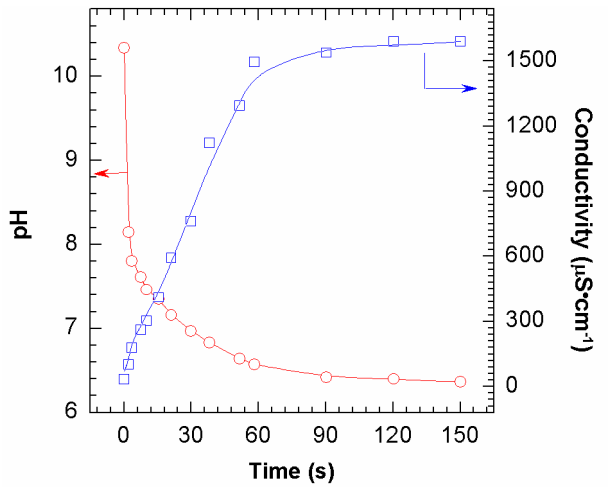

Fig. S4 Evolution of the conductivity and pH of a 100 mM UC22AMPM solution with increasing CO_2 bubbling time.

A series of 20 mL 100 mM UC22AMPM solutions were prepared as described above. CO_2 was bubbled at a flow rate of 0.1 L·min^{-1} for different periods of time. As shown in Fig. S1 and S4, with increasing CO_2 bubbling time, the zero-shear viscosity and conductivity of the 100 mM UC22AMPM solution first dramatically increase, then levels off to a plateau value after ~1 min, accompanied by a decrease in pH from approximately 10.3 to 6.4. Bubbling CO_2 results in the formation of protonated species, which behave as ultra-long carbon chain cationic surfactants. Over time, the amount of protonated species increases. Driven by free-energy minimization,[10-12] these surfactant molecules start to self-assemble into micellar aggregates, which gradually grow into long wormlike micelles and entangle into a dynamic network, conferring high viscoelasticity to the solutions.

After that, air is bubbled into the viscoelastic solution (UC22AMPM-CO_2) at a flow rate of 0.1 L·min^{-1}. As shown in Fig. S5, with increasing air bubbling time, the conductivity of the 100 mM UC22AMPM-CO_2 solution first dramatically decrease, then levels off to a plateau value after ~12 min, accompanied by a increase in pH from approximately 6.4 to 8.56, implying the deprotonation of ionized UC22AMPM, i.e., ultra-long-chain cationic surfactant concentration decreases. Thus, the viscosity of the solution decreases from 300,000 to 3 mPa·s, reflecting the evolution of micellar structures from worm to spherical micelles.

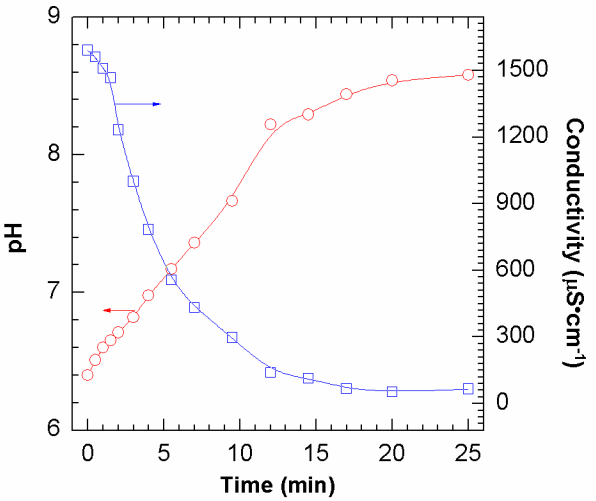

Fig. S5 Evolution of the conductivity and pH of a 100 mM UC22AMPM solution with increasing air bubbling time.

2.4 Measurement of the polarity

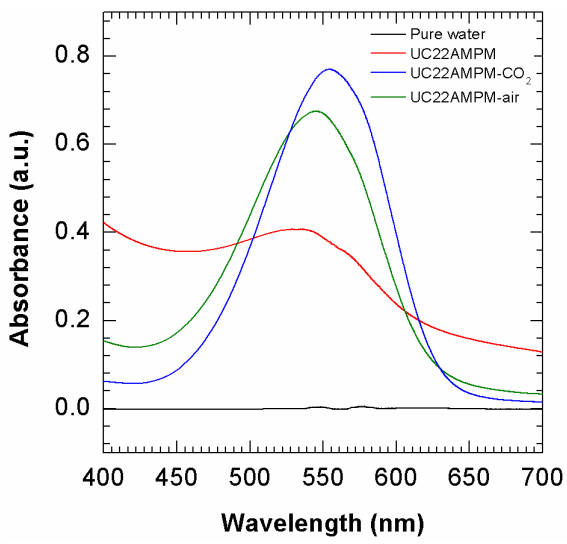

Fig. S6 UV-vis spectrum of Nile red in 10 mM UC22AMPM solution.

An increase in polarity can generally be ascribed to the formation of ionic species, and the polarity change can be measured by using the solvatochromic dye, Nile red, whose wavelength of maximum absorbance, λ_{max}, correlates with solvent polarity and has been used for a variety of solvents.[13] As shown in Fig. S6, λ_{max} is shifted to longer wavelengths by about 19 nm after bubbling CO_2 relative to that before bubbling CO_2, thus confirming an increase in the polarity of the UC22AMPM-CO_2 solutions. In other words, UC22AMPM molecules have acquired charge. After removing CO_2, the polarity decreases (as shown by a shift of λ_{max} by about 10 nm), indicating that some of the ionic species have been deprotonated.

2.5 NMR spectra of UC22AMPM and UC22AMPM-CO_2

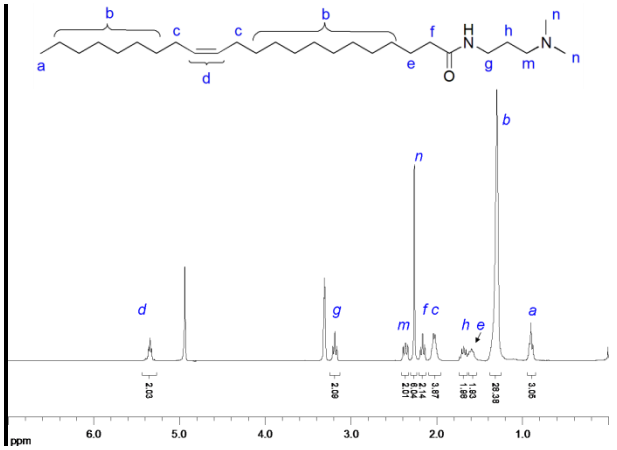

Fig. S7 The original ^{1}H NMR spectrum of UC22AMPM using CD_3OD/D_2O (v/v=5:1) as a solvent.

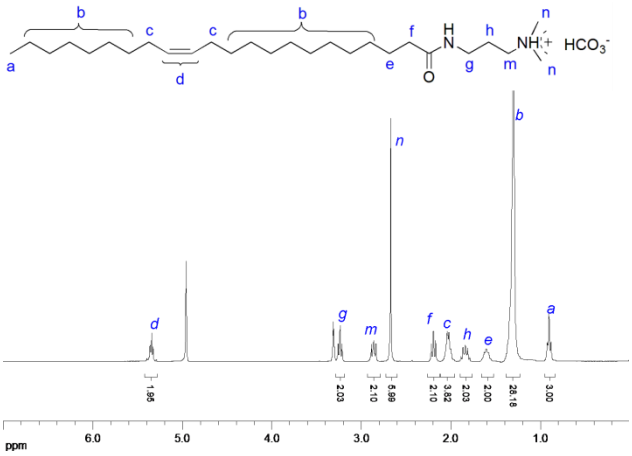

Fig. S8 The original ^{1}H NMR spectrum of UC22AMPM-CO_2 obtained by bubbling CO_2 into UC22AMPM with CD_3OD/D_2O (v/v=5:1) as a solvent.

Through the comparison between Fig. S7 and S8, it is easily found that the chemical shifts of $\boldsymbol{H}^h$, $\boldsymbol{H}^m$ and $\boldsymbol{H}^n$ next to tertiary ***N*** atom shift to low field when UC22AMPM is treated with CO_2. This suggests the chemical environment of $\boldsymbol{H}^h$, $\boldsymbol{H}^m$ and $\boldsymbol{H}^n$ has been changed, i.e., the terminal tertiary amine has been protonated into ionic species.[14]

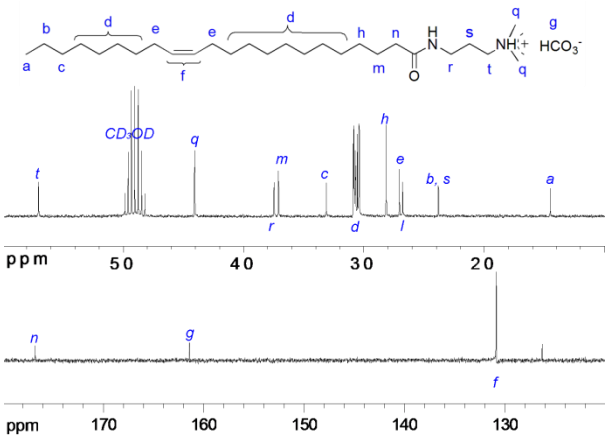

Fig. S9 ^{13}C NMR spectrum of UC22AMPM-CO_2 obtained by bubbling CO_2 into UC22AMPM with CD_3OD/D_2O (v/v=5:1) as a solvent.

In Fig. S9, the signal at ~161 ppm is attributed to the hydrogen carbonate ion according to the results reported by Jessop[14] and Mani et al.[15] Thus, bubbling CO_2 induces the protonation of the terminal tertiary amine group of UC22AMPM, forming ammonium hydrogen carbonate.

2.6 Degree of protonation (δ) of UC22AMPM at different pH values

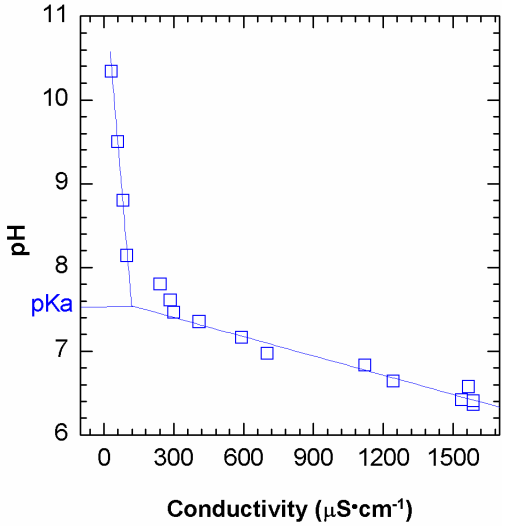

Fig. S10 pH vs conductivity showing the pKa value of UC22AMPM.

The pK_a of UC22AMPM can be obtained by a combined measurement of pH-titration and conductivity. When gradually decreasing the solution pH from 10.3 to 6.4 by using glucono-δ-lactone,[16] a clear inflection point in the conductivity was observed at a pH of 7.56, which thus corresponds to the pK_a of UC22AMPM (Fig. S10). Knowing the value of the pK_a, the degree of protonation (δ) at different pH values can then be calculated from the equation:[16]

$$\delta = \frac{10^{-pH}}{10^{-pH} + 10^{-pK_a}} \qquad (2)$$

Bubbling CO_2 into the solution until equilibrium causes the pH of UC22AMPM solution to decrease from 10.3 to a minimum of 6.4, thus, δ ranges from 0 to an upper critical value of ~0.94. When bubbling air until equilibrium, the pH only reverts back to 8.56, not to the original value, corresponding to a δ of 0.04.

2.7 Critical micellar concentration of UC22AMPM-CO_2

The critical micellar concentration (*cmc*) of UC22AMPM-CO_2 was determined by fluorescence spectroscopy, using pyrene as a probe. Pyrene is widely used as a fluorescence probe, owing to its low solubility in water, long fluorescence lifetime, high sensitivity to the polarity of its microenvironment, and preferential solubilization in hydrophobic microdomains. The vibronic fluorescence spectrum of pyrene exhibits five peaks, and the intensities ratio of the first (I_1) and the third (I_3) vibronic peaks for the emission spectrum provides an estimate of the relative hydrophobicity of the local environment,[17,18] therefore the *cmc* can be obtained from measurements of the change in I_1/I_3 as a function of surfactant concentration. As shown in Fig. S11, upon increasing the concentration of UC22AMPM-CO_2 the intensities ratio I_1/I_3 smoothly decreases, followed by a dramatic drop. The critical value at which I_1/I_3 starts to decline rapidly is the cmc. For this system, the value obtained is ~0.0085 mM, a value quite close to the one reported for EDAS (3-Nerucamidopropyl-N,N-dimethyl ammonium) propane sulfonate, 0.0032 mM)[3] and EDAB (erucyl dimethyl amidopropyl betaine, 0.0076 mM).[19] This implies that UC22AMPM-CO_2 starts self-assembling at a very low concentration, and long flexible wormlike micelles may be generated as the concentration is higher than ~10 times the *cmc*.[12]

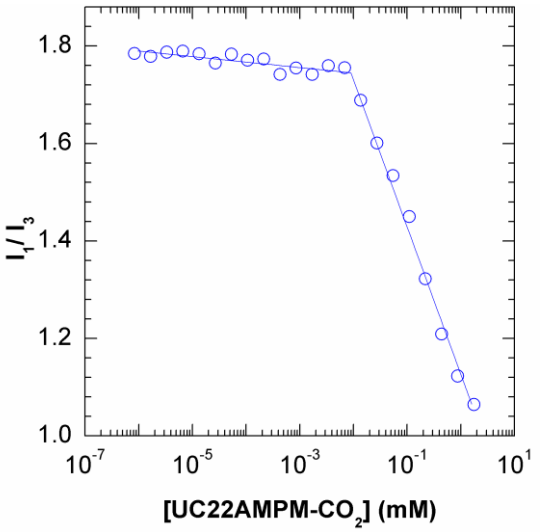

Fig. S11 I_1/I_3 values obtained by fluorescence spectroscopy plotted as a function of UC22AMPM-CO_2 concentration at 25 °C.

References

1. Z. Chu and Y. Feng, *Synlett* **2009**, *16*, 2655.
2. M. E. Cates and S. J. Candau, *J. Phys.-Condes. Matter* **1990**, *2*, 6869.
3. Z. Chu, Y. Feng, X. Su and Y. Han, *Langmuir*, 2010, **26**, 7783.
4. H. Hoffmann, *Adv. Mater.* **1994**, *6*, 116.
5. M. S. Turner and M. E. Cates, *J. Phys. II* **1992**, *2*, 503.
6. S. R. Raghavan and E. W. Kaler, *Langmuir* **2001**, *17*, 300.
7. Y. Han, Y. Feng, H. Sun, Z. Li, Y. Han, H. Wang, *J. Phys. Chem. B* **2011**, *115*, 6893.
8. T. M. Clausen, P. K. Vinson, J. R. Minter, H. T. Davis, Y. Talmon, W. G. Miller, *J. Phys. Chem.* **1992**, *96*, 474.
9. R. Granek, M. E. Cates, *J. Chem. Phys.* **1992**, *96*, 4758.
10. C. A. Dreiss, *Soft Matter*, 2007, **3**, 956.
11. S. R. Raghavan, *Langmuir* **2009**, *25*, 8382.
12. S. J. Candau, R. Oda, *Colloid Surf. A-Physicochem. Eng. Asp.* **2001**, *183*, 5.
13. C. Reichardt, *Chem. Rev.*, 1994, **94**, 2319.
14. S. M. Mercer and P. G.Jessop, *ChemSusChem*, 2010, **3**, 467.
15. (15) F. Mani, M. Peruzzini and P. Stoppioni, *Green Chem.*, 2006, **8**, 995.
16. Q. Yan, R. Zhou, C. Fu, H. Zhang, Y. Yin and J. Yuan, *Angew. Chem.-Int. Ed.*, 2011, **50**, 4923.
17. K. Kalyanasundaram; Thomas, J. K. *J. Am. Chem. Soc.* **1977**, *99*, 2039.
18. F. M. Winnik, S. T. A. Regismond, *Colloid Surf. A-Physicochem. Eng. Asp.*, **1996**, *118*, 1.
19. D. Feng; Y. Zhang; Q. Chen; J. Wang; B. Li; Feng, Y. *J. Surfact. Deterg.* **2012**, *15*, 657.